Available online at www.sciencedirect.com
SCIENCE DIRECT®
Journal of Solid State Chemistry 178 (2005) 2339–2345
JOURNAL OF SOLID STATE CHEMISTRY
www.elsevier.com/locate/jssc

Influence of hydrogen on the magnetic and electrical properties of GdI_2H_x ($0 \leqslant x \leqslant 1$)

Mikhail Ryazanov, Arndt Simon*, Reinhard K. Kremer, Hansjürgen Mattausch

Max-Planck Institut für Festkörperforschung, Heisenbergstr. 1, D-70569 Stuttgart, Germany

Received 18 April 2005; received in revised form 20 May 2005; accepted 20 May 2005

Abstract

We have studied the effect of hydrogen insertion in GdI_2 on its magnetic and electrical properties. The ferromagnetic layered metal GdI_2 reversibly absorbs hydrogen with the formation of GdI_2H_x which exhibits a range of homogeneity $0 \leqslant x \leqslant 1$. These phases crystallize with the hexagonal MoS_2-type heavy atom arrangement. Variation of the hydrogen content is accompanied by a monotonic change in the lattice parameters, and a decreases from 4.074(1) to 4.023(1) Å whereas c increases from 15.050(5) to 15.394(5) Å for $x = 0-0.97$. The molar volume passes through a maximum at $x \approx 0.35$. Magnetization and resistance measurements reveal a substantial change in the physical properties of GdI_2H_x as a function of the hydrogen content, particularly as x approaches a critical value of $\sim 1/3$. The Curie temperature rapidly decreases with increasing hydrogen content, and the long-range magnetic ordering is destroyed for $x > 0.33$. The phases GdI_2H_x with $0.42 \leqslant x \leqslant 0.69$ exhibit characteristics of a spin-glass below the magnetic freezing temperatures $T_f = 24$ and 3 K for $x = 0.42$ and 0.69, respectively. The hydride halides GdI_2H_x ($x > 0.19$) show thermally activated conduction, accompanied by a steep increase of the activation energy at $x \approx 0.33$. The anomalies observed can be understood by assuming an ordering of the hydrogen atoms for $x = 1/3$ within each layer.

Keywords: Gadolinium diiodide; Gadolinium hydride iodides; Magnetic phase transition; Ferromagnetism; Spin-glass behavior; Electrical properties

1. Introduction

Layered diiodides of the rare-earth elements have attracted much attention due to their interesting chemical and physical properties [1–8]. For example, SmI_2 is a one-electron transfer reagent that has found wide application as a selective reducing agent in organic and organometallic synthesis [7,8]. Another remarkable example is gadolinium diiodide [1]. GdI_2 is a narrow d-band metal which orders ferromagnetically close to room temperature and shows a large negative magnetoresistance of ~65% at 300 K in an applied field of $H = 7$ T [9,10]. These extraordinary properties are closely related to the structural and electronic features of GdI_2. The compound crystallizes in the hexagonal 2H-MoS_2 structure type with triangular metal atom layers sandwiched by layers of I atoms (Fig. 1). Such GdI_2 slabs are close-packed along the c-axis via van der Waals interactions.

The magnetic layers which contain formally divalent Gd ions with an electronic configuration $4f^7 5d^1$ are well isolated from each other, suggesting a strong 2D character of both the metallic properties as well as the magnetic coupling. The interactions between localized electrons in the half-filled $4f$ shell and conduction d electrons results in a bulk ferromagnetic (fm) order near room temperature [1,9–13]. Since any spin–orbit coupling is precluded for the Gd^{3+} ions with a spin-only ground state ($^8S_{7/2}$), the spin exchange is considered to be isotropic of the Heisenberg type.

The large magnetoresistance effect has been attributed to a strong spin disorder scattering of the conduction $5d$

*Corresponding author. Fax: +49 711 689 1642.
E-mail address: A.Simon@fkf.mpg.de (A. Simon).

0022-4596/$ - see front matter © 2005 Elsevier Inc. All rights reserved.
doi:10.1016/j.jssc.2005.05.026

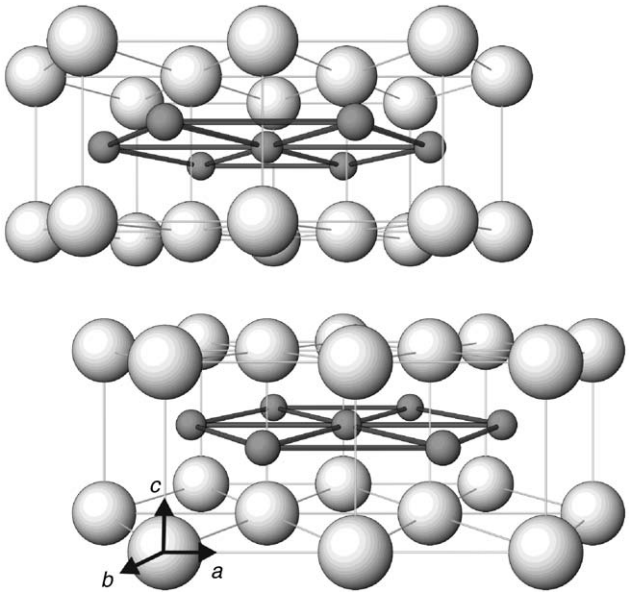

Fig. 1. Perspective view of the crystal structure of GdI_2 along the *b*-axis. Gd and I atoms are depicted with increasing size.

electrons by the localized 4*f* electrons [12]. According to spin-polarized electronic structure calculations [9], the partially filled conduction band has mainly Gd $5d_{z^2}$ character and is almost fully spin-polarized. The electronic density of states shows a van Hove singularity slightly below the Fermi level. From this point of view, it seems particularly interesting to study the physical properties of hole-doped samples, i.e. trying to move the Fermi level closer to the singularity. For this, a localization of the conduction electrons with hydrogen insertion in GdI_2 seemed to be a suitable way. Hydrogenated GdI_2H_x phases in the concentration range $0.28 \leqslant x \leqslant 0.34$ have first been investigated by Michaelis et al. [13]. It has been found that the hydrogen incorporation into GdI_2 results in a successive suppression of the fm order with a decrease of the Curie temperature and thermally activated electrical conduction. From neutron measurements on isostructural $CeI_2D_{0.97}$, the hydrogen atoms were found to occupy the centers of metal atom triangles [14], as is also plausible from chemical bonding arguments [15].

In the present work we have prepared a series of GdI_2H_x samples in the full hydrogenation range ($0 \leqslant x \leqslant 1$) and investigated their magnetic and electrical properties. We find that the system goes from a fm state to a spin-glass behavior at a critical hydrogen concentration $x \approx 0.33$. Furthermore, there is a sharp change in other macroscopic parameters (molar volumes, low-temperature saturation moments, room-temperature resistances) when approaching $x \approx 0.33$.

2. Experimental section

GdI_2 as metallic greenish-gold powder was synthesized by a reaction of sublimed GdI_3 with Gd filings (99.99%; Johnson Matthey, Karlsruhe) at 820 °C for 30 days in tantalum tubes filled with argon and closed by arc welding. To avoid oxidation of the reaction containers, these were sealed in evacuated silica jackets. Hydrogenation experiments were carried out in a Sieverts-type apparatus [16,17] by slowly heating GdI_2 in a closed system under 1 atm H_2 (99.999%; Messer–Griesheim). Increasing the temperature to 650 °C and keeping the samples at that temperature for 5–6 h led to a fully hydrogenated grayish product of analytical composition $GdI_2H_{0.97(3)}$.

Partially hydrogenated samples, GdI_2H_x ($x < 0.97$), were prepared by heating pressed pellets of appropriate quantities of GdI_2 and $GdI_2H_{0.97}$ at 650 °C for 2–3 days in molybdenum ampoules surrounded by Ar-filled silica tubes. To minimize the volume of the silica jacket, an experimental setup described in Ref. [18] was used. The advantage of vanishing gas phase was paid for by an increased silica surface allowing for some hydrogen diffusion. Since the studied compounds are sensitive to air and moisture, all manipulations were performed under inert atmosphere with Schlenk technique (or glovebox, H_2O and O_2 below ~0.2 and ~0.8 ppm, respectively).

The identification of the reaction products and the determination of the lattice parameters were carried out by X-ray powder diffraction on a Stoe Stadi P diffractometer with monochromatic Mo$K\alpha_1$ radiation ($\lambda = 0.7093$ Å, germanium monochromator). The powdered samples were mixed with silicon as an internal standard ($a = 5.4303$ Å) and sealed in glass capillaries filled with Ar.

The hydrogen content *x* in GdI_2H_x was determined by chemical analysis with the Karl Fischer method [19]. Samples (25–50 mg) were mixed with V_2O_5 used as an oxidant and reacted in flowing oxygen at 950 °C. The generated H_2O was then titrated with a Karl Fischer coulometric detector KF 653 (Metrohm) [20]. The hydrogen content was calculated as a mean value from two independent measurements. The maximal spread of *x* calculated for the composition GdI_2H_x was found to amount to $\Delta x = 0.03$.

Measurements of the dc magnetization were performed with a SQUID magnetometer (MPMS, Quantum Design) between 2 and 350 K and magnetic fields *H* up to 70 kOe. The polycrystalline samples were pressed to pellets (diameter 3 mm) and sealed in quartz glass ampoules under 1 atm He exchange gas to provide sufficient thermal contact. Electrical resistances were measured on pressed sample pellets (diameter 5 mm, thickness ~1 mm) by the van der Pauw method [21] in the temperature range 100–300 K. The pellets were

pressed onto four gold-plated spring contacts within a vacuum-tight cell.

3. Results and discussion

Heating GdI_2/GdI_2H reaction mixtures in appropriate quantities results in the formation of GdI_2H_x with a homogeneity range of $0 \leqslant x \leqslant 1$. The difference between sample compositions expected from the reaction stoichiometry and the analytically determined compositions deviates by less than 10%. Variation of the hydrogen content is accompanied by a color change from greenish-gold via dark to light gray as x approaches its upper limit. Like GdI_2, the hydrogenated products crystallize with the hexagonal MoS_2-type heavy atom arrangement. The lattice parameters as a function of hydrogen content x are plotted in Fig. 2. These vary continuously with a significant increase of the c-axis length (0.34 Å), whereas a slightly (0.05 Å) decreases with increasing x. A similar tendency in the lattice parameter variation has been observed in other known LnI_2H_x systems [17,22]. It is worth to note that the molar volume of GdI_2H_x passes a maximum at $x \approx 0.35$ (see Fig. 2), the composition

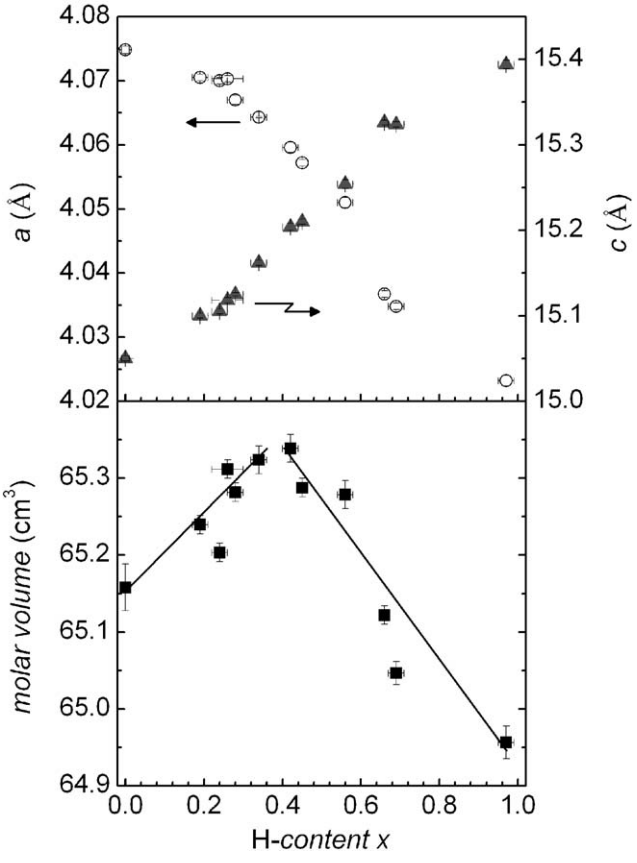

Fig. 2. Lattice parameters and molar volume of GdI_2H_x as a function of hydrogen content (x). The lines are guides for the eye.

Table 1
Curie temperature of GdI_2 as determined from different experimental data

Method	T_C (K)	Reference
dc susceptibility	320–340	1
ac susceptibility	313.0(5)	11
	278(1)[a]	This work
Magnetization	280	13
	290(5)	9
	280(2)[b]	This work
(Arrott plots)	273(1)[c]	This work
	276(2)	10
	286(2)	12
Heat capacity	275(1)	24

[a]From magnetization data measured in an ac magnetic field of 1 Oe.
[b]From dc magnetization data measured in a 100 Oe field.
[c]Curie temperature in zero magnetic field as determined from modified Arrott plots [23].

where also the physical properties undergo a substantial change as will be shown in the following.

GdI_2 is known to order ferromagnetically close to room temperature. However, the values of the Curie temperature T_C reported so far vary in a wide range, from 276 to 320 K [1,9–13]. This marked spread in T_C obviously depends on the preparation and history of samples, as well as the experimental technique and the way of data analysis. In Table 1 we have compiled the results of different experiments to determine the Curie temperature of our GdI_2 samples, compared with known literature data.

As the Curie temperature, we have chosen the temperature where the spontaneous magnetization exhibits the fastest change as a function of temperature. The fm ordering temperature can then be determined from magnetization measurements as a point where the $d\chi(T)/dT$ curve shows a minimum. Applying this approach to the magnetization data measured in low magnetic fields results in $T_C \approx 278-280$ K. A somewhat lower value of ~275 K has been observed from modified Arrott plots [23] and specific heat measurements [24].

Fig. 3 shows the effect of the hydrogen absorption on the fm ordering of GdI_2H_x. The insertion of hydrogen into the metal atom layers results in a steep decrease of the Curie temperature and a smoothing of the magnetization curve. In contrast to GdI_2, the magnetic susceptibilities of the hydrogenated samples with $0 < x \leqslant 0.34$ do not show an abrupt transition any more, but a rather gradual increase upon cooling with saturation at low temperatures. This hampers an accurate determination of the Curie temperature as is evident from diffuse minima in the curves $d\chi/dT$ vs. T (see Fig. 4). The calculated values of T_C for GdI_2H_x are listed in Table 2. Further increase of the hydrogen content leads to the full suppression of the long-range

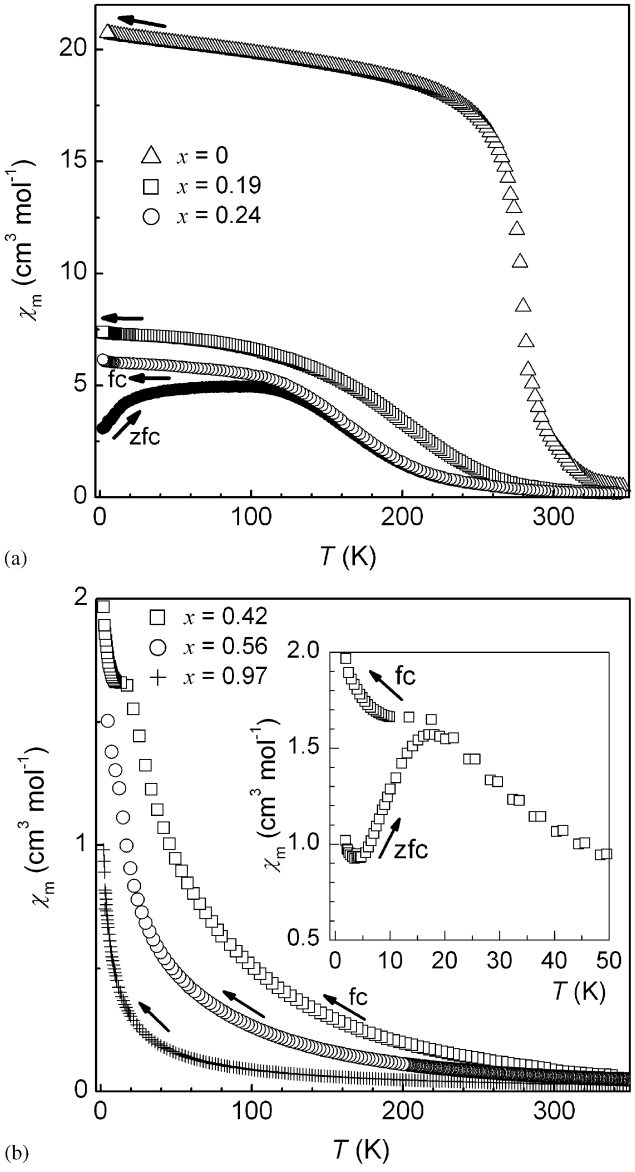

Fig. 3. Temperature dependences of the dc molar magnetic susceptibility (M/H) for GdI_2H_x in the range $0 \leqslant x < 0.3$ (a) and in the range $0.4 < x < 1$ (b), measured in an applied field of 100 Oe (fc—field cooling, zfc—zero field cooling). The insert in (b) shows a comparison of zfc and fc susceptibilities of $GdI_2H_{0.42}$.

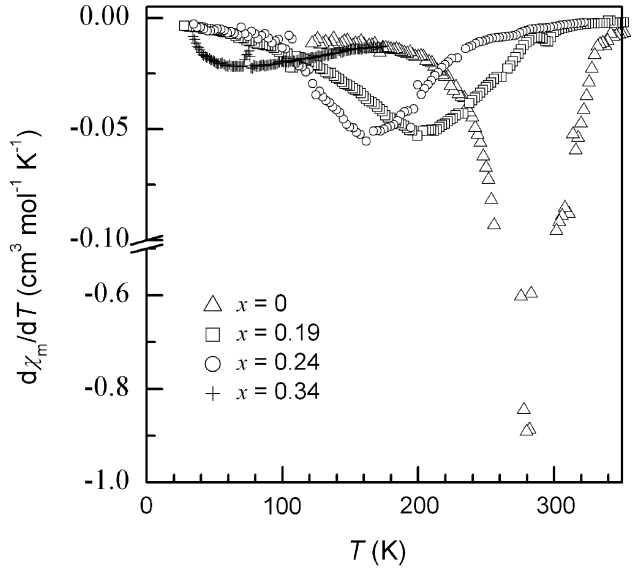

Fig. 4. Temperature gradient of the molar magnetic susceptibility vs. T for the ferromagnetic GdI_2H_x samples ($0 \leqslant x \leqslant 0.34$).

magnetic ordering. The phases GdI_2H_x ($x \geqslant 0.42$) exhibit paramagnetic behavior in field-cooled mode upon lowering the temperature to 2 K (see Fig. 3b).

For the samples with $x < 0.7$ there is a thermal hysteresis in the dc magnetic susceptibilities. As shown for two representative samples in Fig. 3, the $\chi(T)$ curves obtained at different cooling regimes diverge at low temperatures. By cooling in an applied field of 100 Oe (fc), χ_{fc} increases with decreasing T. The magnetic susceptibility of a zero-field-cooled sample measured upon heating after having applied the field at 2 K (zfc) passes a maximum before it merges with the fc curve at high temperatures. Such a splitting between χ_{fc} and χ_{zfc} data is reminiscent of magnetic freezing and is usually observed in spin- and cluster-glasses (mictomagnetism) or in superparamagnetic systems [25]. The spin freezing temperatures, $T_f = (\chi_{zfc})_{max}$, are summarized in Table 2. Ac susceptibility measurements of GdI_2H_x revealed yet another characteristic of spin-glasses, i.e. a maximum in $\chi_{ac}(T)$ and a frequency shift of T_f.

Despite the fact that the Curie temperature rapidly decreases with increasing x, the fm samples GdI_2H_x ($x \leqslant 0.34$), similar to GdI_2 [11,12], do not follow a Curie–Weiss law ($\chi_m = C/T - \theta$) in the paramagnetic state up to 350 K. Although the curves $1/\chi(T)$ in the temperature range 300–350 K can be fitted with a linear function, the analysis results in too high values of the effective magnetic moment ($\mu_{eff} > 10\,\mu_B$). The high-temperature magnetization measurements for $GdI_2H_{0.24}$ clearly indicate that the Curie–Weiss law is obeyed only at very high temperatures ($T > 650$ K) yielding $\theta \approx 380$ K and $\mu_{eff} = 8.3\,\mu_B$, as can be seen in Fig. 5. However, the paramagnetic Curie–Weiss temperatures, θ, evaluated from the data fit in the range $300 < T < 350$ K (see Table 2) allow us to roughly estimate a magnitude of short-range exchange interactions. The Curie–Weiss temperatures of GdI_2H_x are positive ranging from ~450 to 27 K as the hydrogen content increases from $x = 0$ to 0.97. The hydrogen incorporation into GdI_2 leads to a strong suppression of fm coupling, so that the system goes from a fm state to a spin-glass behavior at the critical hydrogen concentration $x \approx 0.33$.

On the other hand, it is striking that even for the samples which display *no* long-range magnetic order, the calculated values $\mu_{eff} > 8.6\,\mu_B$ exceed the theoretical value expected for a system of noninteracting Gd^{3+}

Table 2
Lattice constants and characteristic magnetic parameters for GdI_2H_x (estimated standard deviations are given in parentheses)

Sample	a (Å)	c (Å)	T_C[b] (K)	T_f[c] (K)	θ[d] (K)	M_s(5 K)[f] (μ_B)
GdI_2	4.0750(8)	15.049(3)	280(2)	95(10)	450(6)[e]	7.30
$GdI_2H_{0.19}$	4.0705(5)	15.100(3)	210(10)	85(10)	>250	6.76
$GdI_2H_{0.24}$	4.0700(5)	15.105(3)	170(10)	65(10)	380(5)[e]	6.44
$GdI_2H_{0.34}$[a]	4.0643(5)	15.162(3)	75(10)	30(5)	>260	5.42
$GdI_2H_{0.42}$[a]	4.0596(8)	15.204(4)	—	24(1)	>180	5.40
$GdI_2H_{0.56}$	4.0510(8)	15.254(5)	—	10(1)	>170	5.37
$GdI_2H_{0.69}$	4.0367(5)	15.326(3)	—	3(1)	>60	5.53
$GdI_2H_{0.97}$	4.0232(8)	15.394(5)	—	—	27(1)	5.43

[a]A small contribution from Gd impurities to the magnetic data has been detected, which could be substantially suppressed in a field of 10 kOe.
[b]$T_C = (d\chi_m/dT)_{min}$.
[c]$T_f = (\chi_{zfc}(T))_{max}$.
[d]Values for θ, unless those marked with d, have been evaluated from the Curie–Weiss fits of the χ^{-1} (T) curves (measured at $H = 10$ kOe) in the temperature range $300\,K < T < 350\,K$.
[e]From high-temperature data (650–750 K).
[f]Magnetization moments at $H = 70$ kOe.

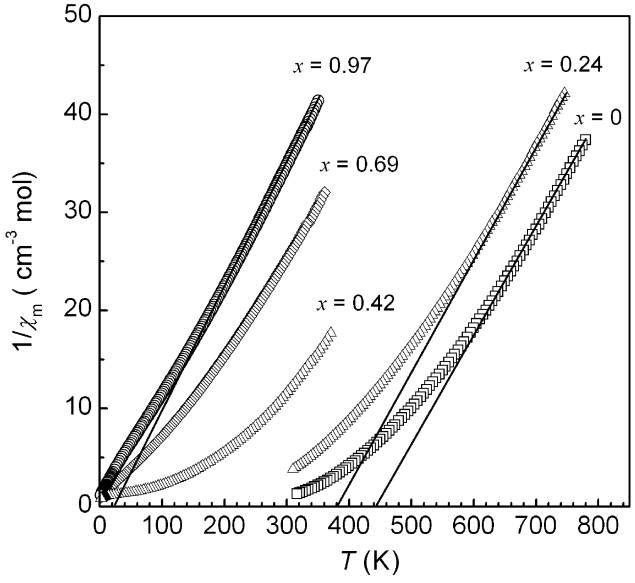

Fig. 5. Inverse χ_{fc} (measured in 10 kOe field) vs. temperature for GdI_2H_x. The solid lines correspond to Curie–Weiss fits of the high-temperature data; fit parameters are in Table 2.

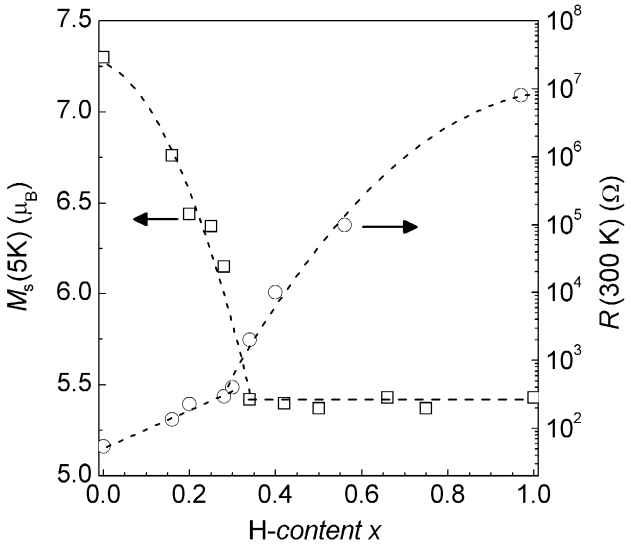

Fig. 6. Saturation magnetic moments $M(H = 70$ kOe) at 5 K and room-temperature resistivities of GdI_2H_x as a function of hydrogen content (x). The lines are guides for the eye.

ions ($S = 7/2$, $\mu_{eff} = 7.94\,\mu_B$) reflecting local fm correlations that are still relevant up to 350 K. Only in the case of large hydrogen concentration ($x \geqslant 0.78$) a fit of the high-temperature magnetic data ($250 < T < 350$ K) to the Curie–Weiss law leads to $\mu_{eff} = 7.93-7.97\,\mu_B$ in good agreement with a value of $7.94\,\mu_B$, expected for the effective moment of the free Gd^{3+} ions.

The observed spin-glass characteristics for quasi-2D Heisenberg systems GdI_2H_x ($0.42 \leqslant x \leqslant 0.69$) imply the coexistence of competing ferro- and antiferromagnetic (afm) interactions besides disorder. It is interesting to note that the disorder is introduced in the diamagnetic H sublattice. The presence of the afm interactions is further corroborated by measurements of the low-temperature magnetization curves. Table 2 contains the saturation magnetization values of GdI_2H_x, M_s, at 5 K in an external field of 70 kOe. For pure GdI_2, the saturation moment is $\sim 7.3\,\mu_B$ consistent with previous experiments [9]. The excess of $0.3\,\mu_B$ as compared to the spin-only moment of the Gd $4f^7$ shell ($7\,\mu_B$) has been attributed to a strong polarization of the $5d$ conduction electrons [9]. With insertion of hydrogen into GdI_2, M_s rapidly decreases from 7.3 to $5.4\,\mu_B$ when x approaches the critical concentration of ~ 0.33, to remain, surprisingly, almost unchanged by further increase of the hydrogen content (see Fig. 6). Thus, the low-temperature saturation moments of GdI_2H_x ($x > 0$) lie below the value expected for a parallel alignment of the Gd^{3+}

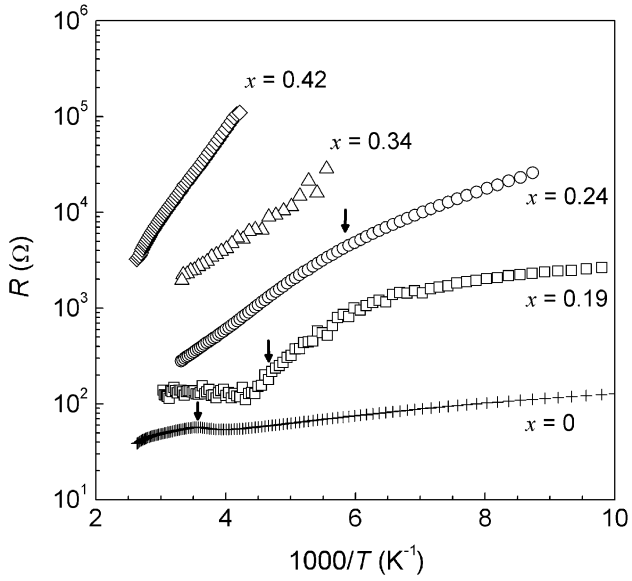

Fig. 7. Electrical resistance of GdI_2H_x as a function of reciprocal temperature. Indicated by arrows are the magnetic transition temperatures.

moments, indicating that afm interactions progress with increasing x.

Fig. 7 displays the electrical resistances of GdI_2H_x as a function of reciprocal temperature. GdI_2 shows metallic behavior, passing through a broad maximum at the Curie temperature. Below ~240 K there is an upturn in the resistance towards low temperatures, in agreement with the previous results [13]. It should be noted that this resistance increase is substantially suppressed by applying a strong magnetic field, e.g. in $H = 50$ kOe. Hence, the resistance anomaly observed at low temperatures appears to be essentially magnetic in nature.

The H-containing samples, GdI_2H_x ($x \geqslant 0.24$), exhibit thermally activated conduction with an increasing resistance upon lowering the temperature. For the fm samples with $x < 0.34$, the resistivity increase is accompanied by a change of the activation energy at the magnetic transition since the $\ln R$ vs. $1/T$ curves change slope near T_C (see Fig. 7). The resistance of $GdI_2H_{0.19}$ is almost constant at high temperatures, and shows a steep rise around the magnetic transition with saturation at lower temperatures ($T = 100-150$ K).

Similar to the magnetic properties, there is a sharp change in the electrical properties of GdI_2H_x near the critical hydrogen content $x \approx 1/3$. As shown in Fig. 6, the room-temperature resistance values lie in almost the same range for $x < 0.33$, whereas these steeply increase for samples with higher hydrogen content. Also the activation energies, E_a, derived from fitting the high-temperature $R(T)$ data ($200 < T < 300$ K) to an Arrhenius law, $R = R_o \exp(E_a/kT)$, change markedly from ~90 to ~185 meV when x increases from 0.34 to 0.42 in comparison with $E_a \approx 90-98$ meV for $x = 0.24-0.34$. A steep increase of resistance at $x \approx 0.33$ has also been found in the related CeI_2H_x system, for which, however, there is a miscibility gap in the range $0 < x < 0.33$ [13].

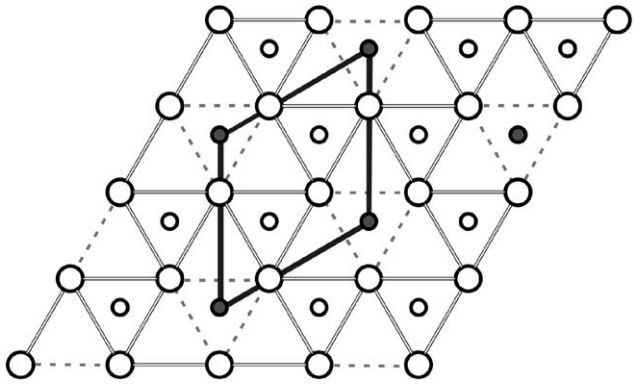

Fig. 8. Schematic representation of an ordering of hydrogen atoms (filled circles) within the Gd atom layer (large circles) for $GdI_2H_{0.33}$, resulting in a 2D superstructure with the unit cell outlined. The solid and the dashed bonds stand for fm and afm interactions in Gd_3 and Gd_3H clusters, respectively.

The magnetic and electrical anomalies observed for GdI_2H_x when approaching the critical hydrogen content x of ~0.33 can be understood along the line of a 2D ordering of the hydrogen atoms for $x = 1/3$, as sketched in Fig. 8. In metallic GdI_2, the fm coupling between the Gd moments within a layer is mediated by an indirect RKKY exchange via the conduction electrons, which are involved in $M-M$ bonding. Insertion of hydrogen into the trigonal metal atom layers has the consequence that a part of the conduction electrons becomes localized at hydride ions. The spin–spin coupling between the metal ions in such "filled" Gd_3H clusters is likely due to direct $f-f$ exchange or superexchange via the H^- ions, which, according to the Goodenough–Kanamori rules [26,27], are expected to be afm for *non-orthogonal* and *half-occupied* magnetic orbitals. The presence of afm clusters in an fm matrix leads to a local spin frustration, yielding magnetic freezing processes at low temperatures. On the other hand, the ordering of Gd_3H clusters for $x = 1/3$ (see Fig. 8) would result in a *fully* frustrated spin configuration, since now competing fm and afm interactions act on each magnetic moment. As a result, the long-range order breaks down, and the samples GdI_2H_x ($0.42 \leqslant x \leqslant 0.69$) exhibit a spin-glass behavior. It should be emphasized that $x = 1/3$ is the *first* hydrogen concentration at which each Gd ion experiences mixed magnetic interactions, yielding a frustrated ground state. By further increase of the hydrogen content there is a change in the ratio of fm and afm interactions, whereas the spin configuration remains frustrated. Moreover, the boundary case, i.e. an antiferromagnetically coupled triangular lattice, is a remarkable example of a geometrical frustrated system [28].

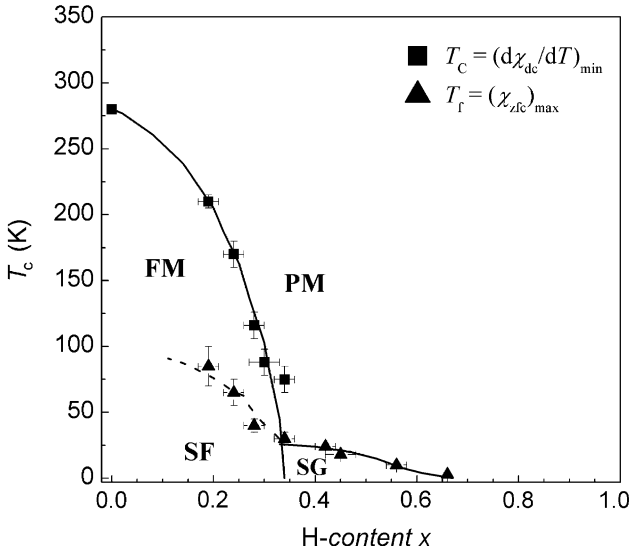

Fig. 9. Magnetic phase diagram of GdI_2H_x. FM, PM, SG and SF indicate ferromagnetic, paramagnetic, spin-glass and spin freezing behavior, respectively.

The positive value of the Curie–Weiss temperature evaluated from the high-temperature data for $GdI_2H_{0.97}$ remains puzzling, as afm correlations would have been expected to dominate for the fully hydrogenated sample. However, this value becomes negative ($\theta \approx -14$ K) for the temperature range 20–100 K, suggesting the prevalence of afm interactions at low temperatures.

4. Conclusion

In summary, the insertion of hydrogen in GdI_2 leads to a drastic change in the magnetic and the electrical properties of GdI_2H_x as x approaches the critical concentration of ~0.33. In Fig. 9, we have presented a tentative magnetic phase diagram derived from the magnetic data described above. With increasing hydrogen concentration, there is a magnetic phase transition at the critical value $x \approx 0.33$. The samples with the low hydrogen content ($x < 0.33$) show a partially fm transition at high temperature, followed by a freezing of fm clusters at low temperature. For higher H concentrations, one observes a spin-glass behavior due to the presence of competing fm and afm interactions.

Acknowledgments

We would like to thank E. Brücher and G. Siegle for expert experimental assistance. We are grateful to Dr. K. Ahn for communicating some early experimental results.

References

[1] J.E. Mee, J.D. Corbett, Inorg. Chem. 4 (1965) 88–93.
[2] J.H. Burrow, C.H. Maule, P. Strange, J.N. Tothill, J.A. Wilson, J. Phys. C 20 (1987) 4115–4133.
[3] G. Meyer, Chem. Rev. 88 (1988) 93–107.
[4] O. Jepsen, O.K. Andersen, Z. Phys. B 97 (1995) 35–47.
[5] K. Stöwe, S. Tratzky, H.P. Beck, A. Jungmann, R. Claessen, R. Zimmermann, G. Meng, P. Steiner, S. Hüfner, J. Alloys Compounds 246 (1997) 101–110.
[6] M.N. Bochkarev, Coord. Chem. Rev. 248 (2004) 835–851.
[7] P. Girard, J.L. Namy, H.B. Kagan, J. Am. Chem. Soc. 102 (1980) 2693–2698.
[8] G.A. Molander, Chem. Rev. 92 (1992) 29–68.
[9] C. Felser, K. Ahn, R.K. Kremer, R. Seshadri, A. Simon, J. Solid State Chem. 147 (1999) 19–25.
[10] K. Ahn, C. Felser, R. Seshadri, R.K. Kremer, A. Simon, J. Alloys Compounds 303–304 (2000) 252–255.
[11] A. Kasten, P.H. Mueller, M. Schienle, Solid State Commun. 51 (1985) 919–921.
[12] I. Eremin, P. Thalmeier, P. Fulde, R.K. Kremer, K. Ahn, A. Simon, Phys. Rev. B 64 (2001) 064425–064426.
[13] C. Michaelis, W. Bauhofer, H. Buchkremer-Hermanns, R.K. Kremer, A. Simon, G.J. Miller, Z. Anorg. Allg. Chem. 618 (1992) 98–106.
[14] C. Michaelis, Hj. Mattausch, H. Bormann, A. Simon, Z. Anorg. Allg. Chem. 607 (1992) 29–33.
[15] Y. Tian, T. Hughbanks, Inorg. Chem. 32 (1993) 400–405.
[16] A. Sieverts, Z. Metallk. 21 (1929) 37–46.
[17] C. Michaelis, Hj. Mattausch, A. Simon, Z. Anorg. Allg. Chem. 610 (1992) 23–27.
[18] A. Simon, K. Trübenbach, H. Borrmann, J. Solid State Chem. 106 (1993) 128–133.
[19] K. Fischer, Angew. Chem. 48 (1935) 394–396.
[20] R. Eger, Hj. Mattausch, A. Simon, Z. Naturforsch. 48b (1993) 48–51.
[21] L.J. van der Pauw, Philips Res. Rep. 13 (1958) 1–9.
[22] M. Ryazanov, A. Simon, Hj. Mattausch, Z. Anorg. Allg. Chem. 630 (2004) 104–108.
[23] A. Arrott, J.E. Noakes, Phys. Rev. Lett. 19 (1967) 786–789.
[24] M. Ryazanov, Ph.D. Thesis, Universität Stuttgart, 2004.
[25] J.A. Mydosh, Spin Glasses: An Experimental Introduction, Taylor and Francis, London, 1993.
[26] J.B. Goodenough, Phys. Rev. 100 (1955) 564–573.
[27] J. Kanamori, J. Phys. Chem. Solids 10 (1959) 87–98.
[28] A.P. Ramirez, Annu. Rev. Mater. Sci. 24 (1994) 453–480.